Combined Electrochemical and EPR Studies of Manganese Schiff Base Complexes Encapsulated within the Cavities of Zeolite Y

Antonio Doménech,[a] Pilar Formentin,[b] Hermenegildo García,*[b] and María J. Sabater*[b]

Keywords: Manganese / Electrochemistry / Zeolites

Encapsulation of manganese(III) and manganese(V) Schiff base complexes within the cavities of zeolite Y has been accomplished by means of established synthetic procedures. The samples have been characterized by a combination of various analytical and spectroscopic techniques that probe either the bulk encapsulated complexes or the species present in the outermost layers of the zeolite grains. Importantly, whereas EPR measurements indicated that aerial oxidation had transformed only about 15–20% of the initially present Mn^{II} cations to Mn^{III}, electrochemical techniques revealed a predominance of Mn^{III} at the external surface. This striking result is due to the fact that electrochemical techniques specifically probe the fraction of electroactive species present in the outermost layers of the zeolite particles. In view of the fact that these complexes are the most accessible and active in heterogeneous catalytic reactions in the liquid phase, the voltammetric measurements provide important information concerning the specific evolution of the reversible Mn^{III}/Mn^{II} redox couple near the surface of the zeolite particles. Furthermore, the unequivocal electrochemical detection of intra-zeolite Mn^{V} species (not observable by EPR spectroscopy) highlights the importance of combining surface characterization tools (electrochemistry) with conventional spectroscopic techniques (IR, UV/Vis, and EPR) of the bulk particle in order to assess the differing nature and distribution of the entrapped transition metal complexes.

Introduction

Immobilization of transition metal complexes within the supercages of X- and Y-type zeolites has been a topic of intense research in recent years, the aim being to produce materials that combine the activity of a molecular catalyst with the sieving capability and ease of separation from the reaction mixture of a microporous solid support.[1–3] One of the most extensively studied systems has been zeolite Y encapsulated (salen)manganese(III) complexes, which have served as efficient epoxidation catalysts in both the homogeneous and heterogeneous phases.[4–7] The incorporation of such catalysts within microporous solids by so-called "ship-in-a-bottle" syntheses basically requires the manipulation of Mn^{II} salts, complex formation, and ulterior oxidation to Mn^{III} by molecular oxygen. In order to gain a detailed knowledge of these hybrid materials and to characterize the intra-zeolite complexes, a set of complementary techniques is required. Routine IR spectroscopy can give information on the intra-zeolite assembly process by probing mainly the organic ligand moiety. However, it cannot reliably distinguish between different metal oxidation states and does not give information about any residual populations of uncomplexed manganese ions that may be present. This is not the case with EPR spectroscopy and electrochemistry, since these techniques can be suitably applied to provide information on the oxidation state and redox chemistry of specific metal ions. This gives them a distinct advantage over other analytical tools. In the case under consideration here, Mn^{II} is EPR-active whereas Mn^{III} is EPR-inactive. Thus, for a given total amount of manganese, the oxidation of Mn^{II} to Mn^{III}, either complexed or uncomplexed, can be conveniently followed by monitoring the decrease in the area of the Mn^{II} EPR signal. This provides information relating to the bulk material.

On the other hand, electrochemical techniques specifically probe the fraction of electroactive species residing in the outermost layers of the zeolite grains. This is due to the fact that, on the time scale of the electrochemical measurement, the diffusion of the accompanying electrolyte that is necessary to maintain the electroneutrality of the solid only occurs to a shallow depth in the zeolite particles.[8–10] Nevertheless, the electrochemical response provides information not only on the oxidation state of the manganese ions, but also on the coordination of the metal center, since the redox potential of the complex has a distinctive value. In practice, the specific information concerning the complexes located in the external layers is very useful since, being most accessible to reagents, these complexes are the most active in heterogeneous catalysis. On the other hand, the population of complexes located at or near the external surface is also more likely to differ from that of the bulk encapsulated complexes in terms of the distribution of metal ion oxidation states. Thus, while spectroscopy gives information on the global population of complexes (i.e. those predominantly located in the internal pores), it might well be that a given catalytic activity is due almost exclusively to the distinct fraction at the outermost sites. Thus,

[a] Departamento de Química Analítica, Universidad de Valencia, Dr. Moliner, 50, 46100 Burjassot, Valencia, Spain
[b] Instituto de Tecnología Química UPV-CSIC, Universidad Politécnica de Valencia, Apartado 22012, 46071 Valencia, Spain
Fax: (internat.) + 34-96/387-7809
E-mail: hgarcia@qim.upv.es

  1434–1948/00/0606–1339 $ 17.50+.50/0

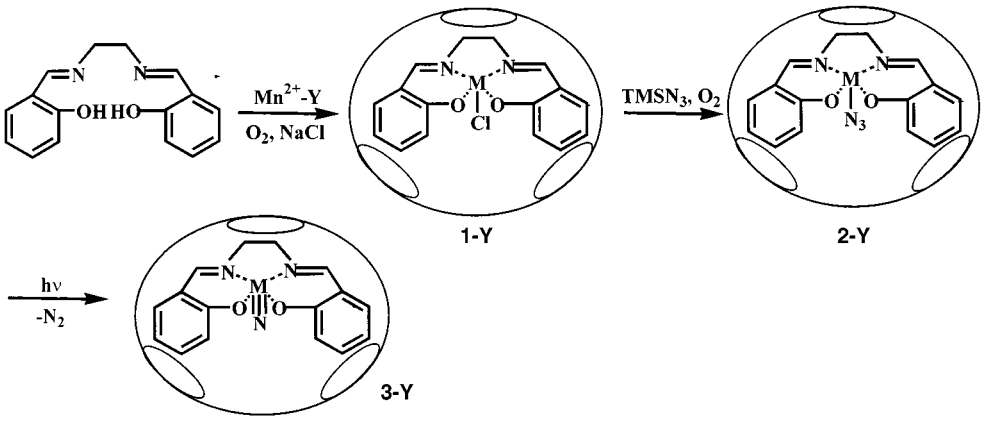

Scheme 1. Preparation of salen-derived manganese(III) and manganese(V) Schiff base complexes in the supercages of zeolite Y

with the aim of obtaining a quantitative estimation of the amount and distribution of Mn^{II}, Mn^{III}, and Mn^{V} species through the zeolite, we have prepared various salen-derived Mn^{III} and Mn^{V} complexes in the cavities of zeolite Y. Whereas EPR measurements and electrochemical techniques were indicative of significant differences in the Mn^{II}/Mn^{III} ratio between the bulk and the external layers, Mn^{V} species were detected only by cyclic voltammetry. This study highlights the importance of combining spectroscopic techniques with surface-specific analytical tools in differentiating between different populations of entrapped complexes.

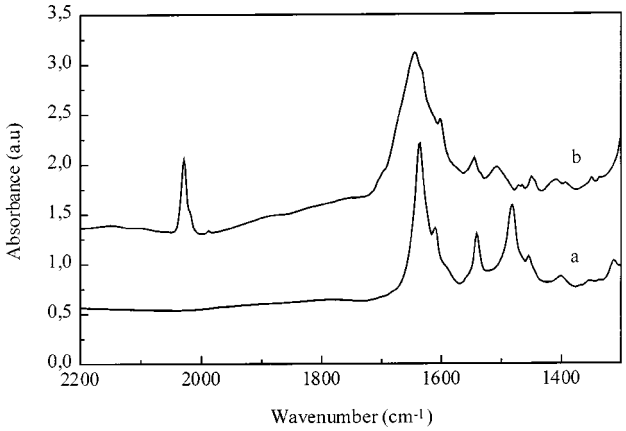

Figure 1. IR spectra of heterogeneous complexes (a) **1-Y** and (b) **2-Y**; the spectra were recorded at room temperature after heating at 100 °C and degassing at 10^{-5} mbar for 1 h

Results and Discussion

Encapsulation of the (salen)Mn complex [salen = 1,2-bis(salicylidenimino)ethylene] within the cavities of zeolite Y, to give **1-Y**, was achieved by treatment of Mn^{2+}-pre-exchanged zeolite Y (0.48% Mn^{2+}; 1 Mn^{2+} every 5 supercages) with the pre-synthesized ligand 1,2-bis(salicylideniminoethylene), followed by treatment with molecular oxygen. As we reported previously, ulterior treatment of **1-Y** with trimethylsilyl azide ($TMSN_3$) allowed access to **2-Y** (Scheme 1).[11] After removal of the excess salen ligand by Soxhlet extraction with dichloromethane, the resulting complexes **1-Y** and **2-Y** were characterized by direct comparison of their DR and IR spectra with those of the corresponding unsupported complexes (**1** and **2**), which were synthesized independently according to previously described methods.[13] The most salient spectroscopic features supporting the formation of **1-Y** were a characteristic imine stretching vibration at 1615 cm^{-1} and a band typical of metallosalen complexes at 1535 cm^{-1}. In the case of **2-Y**, an additional sharp IR absorbance due to the azide ligand at 2037 cm^{-1} confirmed the formation of this heterogenized complex (Figure 1).[11] The corresponding encapsulated nitride complex **3-Y** was obtained by photochemical denitrogenation of the (azido)metal complex **2-Y** as we have reported previously.[11] The transformation of **2-Y** into **3-Y** could be conveniently monitored by IR and Raman spectroscopies, by following the disappearance of the intense azide stretching vibration in the IR spectrum and the concomitant increase in the Raman absorption band characteristic of an Mn≡N triple bond.

The electrochemistry of the related pure complex (salen)$Mn^{III}Cl$ **1** in solution (CH_3CN, DMSO) has been thoroughly studied and essentially involves a reversible one-electron process at a formal potential close to −0.20 V vs. SCE.[8] On the other hand, the cyclic voltammogram for the parent (azido)manganese(III) complex **2**, immobilized on a polymer-film electrode and immersed in neutral aqueous or CH_3CN solution, shows a one-electron reversible couple (C_1/A_1) close to −0.25 V vs. SCE (Figure 2). In both cases, the absence of additional peaks in the +0.8 to −1.0 V potential range indicates that there is no significant dissociation of the complex.

As expected on the basis of previous literature reports, the electrochemical responses obtained for the respective zeolite-modified electrodes **1-Y** and **2-Y** have common features with the patterns and potential values observed for the species in solution and in polymer-film-modified

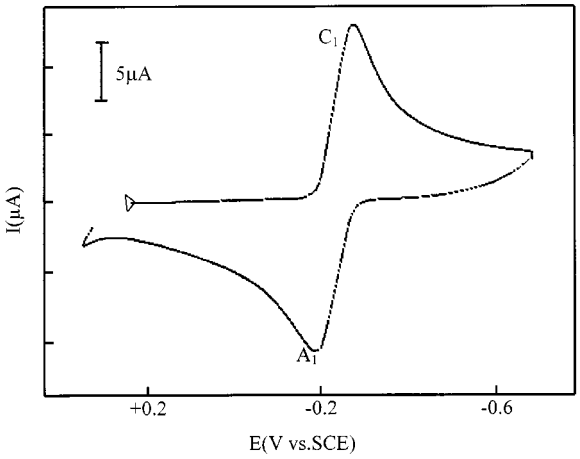

Figure 2. Cyclic voltammogram of a polymer-film-modified electrode of the (salen)MnN_3 complex immersed in H_2O (0.15 M $NaClO_4$); v = 20 mV/s

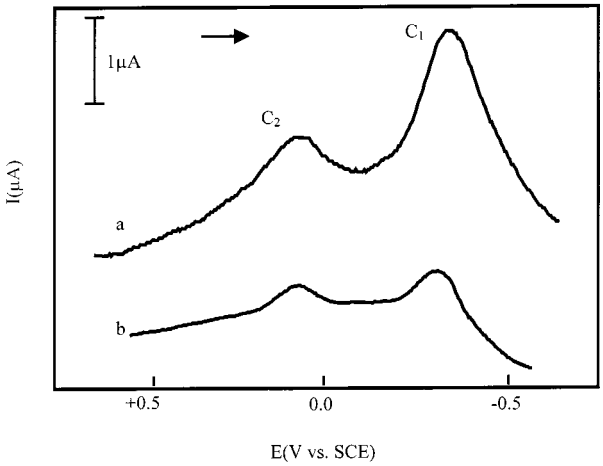

Figure 4. Differential pulse voltammograms of a zeolite-modified electrode containing **2-Y** immersed in H_2O (0.15 M $NaClO_4$); (a) first and (b) second scan; v = 10 mV/s, ΔU = 80 mV

electrodes.[14−16] In fact, both heterogeneous complexes **1-Y** and **2-Y** showed the C_1/A_1 redox couple around −0.25 V vs. SCE together with an additional cathodic peak (C_2) in the +0.3 to −0.2 potential range (Figures 3 and 4). Although comparison of the peak profiles of C_1/A_1 and C_2 suggests that they are similar, no conclusions can be drawn concerning the relative number of electrons transferred in the two processes since the populations of the relevant species are likely to be very different. The (azido)manganese(III) complex **2-Y** showed an additional two-electron oxidation process (A_3) at +0.30 V vs. SCE (Figure 3).

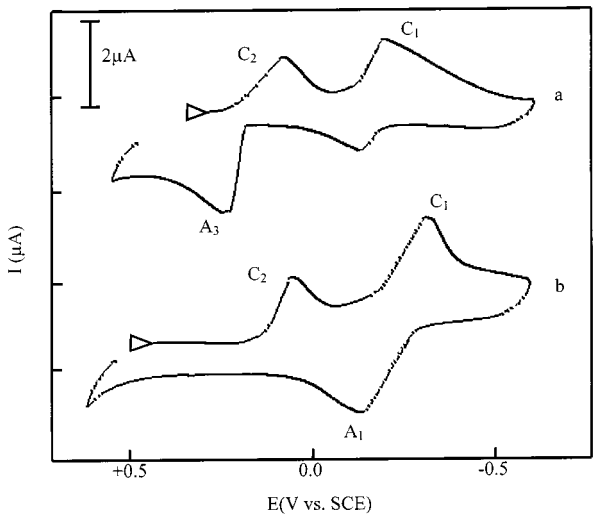

Figure 3. Cyclic voltammograms of zeolite-modified electrodes containing (a) **2-Y** and (b) **1-Y** in aqueous media (0.15 M $NaClO_4$); v = 20 mV/s

Assignment of these redox processes can be partly achieved on the basis of the electrochemical responses observed for the respective non-supported complexes. Thus, the C_1/A_1 couple clearly corresponds to redox transformations affecting those Mn(salen)X (X = Cl^-, N_3^-) complexes located in the boundary sites of the zeolite surface as indicated in eq. 1, where s represents species in the solution phase, b represents adsorbed boundary species, and M^+ is the charge-balancing cation of the salt acting as the supporting electrolyte.[14−16]

$$(salen)Mn^{III}X\,(b) + M^+(s) + e^- \rightarrow (salen)Mn^{II}X\,(b) + M^+(b) \qquad (1)$$

On the other hand, the C_2 process is also observed as a single peak in the electrochemical response of the original Mn-Y sample prior to addition of the ligand. Thus, this peak cannot correspond to any manganese Schiff base complex, but rather to other manganese species present in the outermost layers. These adventitious Mn species are most probably small oxide clusters deposited at the zeolite surface, which would not participate in the complexation.

Finally, the third redox peak A_3 can most probably be attributed to free azide ligands N_3^-. Strong support for this assignment is provided by the observations that: (i) the A_3 peak is not observed on scanning the electrochemical response of the parent complex **1-Y**, and (ii) an aqueous solution of NaN_3 shows an oxidation peak at the same potential. While azide N_3^- displacement from complex **2** by other ligands or solvent cannot be ruled out, the appearance of this specific N_3^- peak can more probably be attributed to residual traces of azido compounds employed in the synthesis of **2**.

Quantification of the Mn^{II}/Mn^{III} ratio present in electrochemically probed sites of the zeolite particle was accomplished by comparing the experimental data with theoretical voltammetric curves. These theoretical simulations were obtained by dividing the intensities of the first and second scans of the anodic peak (I'_{ap}/I''_{ap}) and assuming single reversible redox processes and equal diffusion coefficients for the species involved in the oxidation and reduction processes.[17] Although these measurements are subject to relatively large errors (25%), our estimates of the initial amount of Mn^{III} present in the non-exchanged samples was 45% for **1-Y** and 55% for **2-Y**. Furthermore, when samples of **1-Y** and **2-Y** were submitted to supplementary ion-exchange with NaCl, which supposedly replaces uncomplexed Mn^{2+} by Na^+, the proportion of Mn^{III} increased to 85% and 90% in the samples of **1-Y** and **2-Y**, respectively (the amounts of

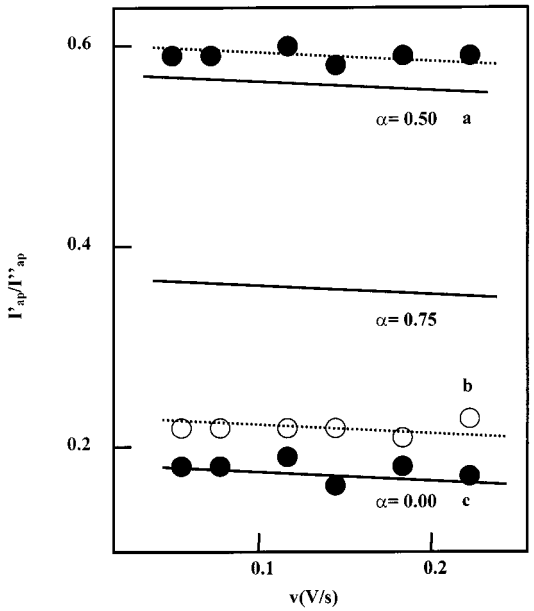

Figure 5. Comparison between theoretical and experimental plots of anodic peak intensity ratios of the first and second scans (I'_{ap}/I''_{ap}) vs. potential scan rate in CVs of different modified electrodes: (a) **2-Y** before treatment with 1 M NaCl; (b) **2-Y** after ion exchange with 1 M NaCl, and (c) pure complex **2**; the dotted lines correspond to experimental data for the supported complexes; α denotes the Mn^{II}/Mn^{III} molar fraction

Mn^{III} calculated to be present in the pure complex **2** and the supported complex **2-Y** before and after ion-exchange are represented in Figure 5).

In striking contrast, EPR measurements comparing the relative intensities of the signals before and after oxidative treatment indicated that a high proportion of the initial Mn^{II} cations of the bulk particle remained unaltered. We estimate that only about 15−20% (error 10%) of the initially present Mn^{II} cations were oxidized to Mn^{III} in both the encapsulated complexes **1-Y** and **2-Y**, reflecting the difficulty in achieving complete oxidation within the zeolite cavities.[18−20] Although absolute quantitative EPR measurements are subject to relatively large experimental errors compared to more accurate chemical analysis, we found the aforementioned ratio of oxidation states to be readily reproducible between samples examined under exactly the same conditions by EPR. Hence, this apparent contradictory result [predominant Mn^{II} by EPR but no detectable (salen)Mn^{II} complexes by cyclic voltammetry] can only be reconciled by considering that only a fraction of the total loading is really probed by cyclic voltammetry (the maximum total charge uptake was found to be 10^{-4} coulomb/mg zeolite, i.e. 10^{-9} mol e^-/mg zeolite, which roughly corresponds to 1.1% of the total complex calculated by chemical analysis). In fact, although the actual mechanisms of intrazeolite electrochemical processes remain controversial, a consensus has been reached that the electrochemical response is exclusively due to those species located in the outermost supercavities.[14−16] To obtain experimental support for the prevalence of Mn^{III} over Mn^{II} at the most exposed layers of the zeolite grains, we also measured the XPS of **1-Y**. As expected, and in accordance with the electrochemical measurements, the electronic transition at 641.7 eV, characteristic of the 2p orbital of Mn^{III} ($Mn2p_{(3/2)}$) predominated, whereas that corresponding to Mn^{II} (the characteristic satellite peak of its 2p orbital appears around 647 eV) was virtually absent.

Finally, the differential pulse voltammetric curve (DPV_s curve) of the irradiated zeolite **3-Y** featured an additional cathodic peak C_4 at +0.65 V, which, on the basis of its redox potential, could be assigned to reduction of the nitridomanganese(V) species generated photochemically from the corresponding Mn^{III} azide precursor complex (Figure 6). Since the current associated with this peak was comparable to that associated with the prior redox processes in the **2-Y** precursor, it seems reasonable to conclude that upon irradiation a significant amount of the (salen)$Mn^{III}N_3$ was transformed into the high-valent Mn^V complex, at least in the outermost layers of the particles. This interpretation is also in agreement with previous IR and Raman studies, which showed a disappearance of the N_3 stretching vibration at 2039 cm^{-1} and a concurrent appearance of the nitrido N≡M band upon irradiation.[11] We recorded an EPR spectrum of the sample under consideration here. However, in the present case, EPR spectroscopy was unable to detect the formation of any Mn^V species since the intense signal due to the residual Mn^{II} ions in the bulk zeolite completely masked any weaker signals due to the high-valent manganese complex that may have been present.

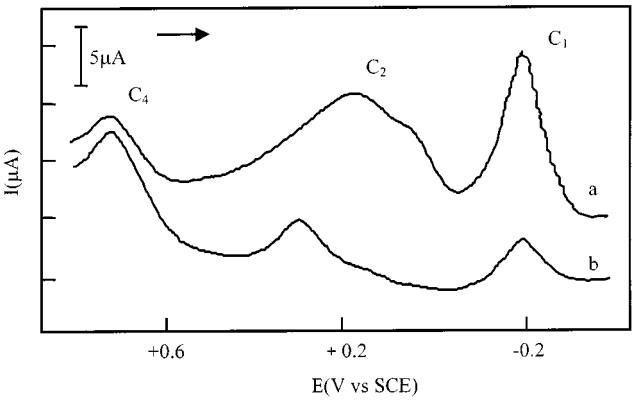

Figure 6. Differential pulse voltammograms (DPVs) for a zeolite-modified electrode containing the **3-Y** complex immersed in H_2O (0.15 M $NaClO_4$); (a) first and (b) second scan; v = 10 mV/s, ΔU = 80 mV

Conclusion

According to the data derived from the electrochemical measurements, the manganese Schiff base complexes **1-Y**, **2-Y**, and **3-Y** residing in the outermost layers of the zeolite Y particles have the oxidation state that would be expected on the basis of literature reports concerning the preparation of unsupported complexes **1**−**3**. Moreover, cyclic voltammetry and differential pulse voltammetry have confirmed the presence of coexisting Mn^{III} and Mn^V species in the supported (nitrido)manganese(V) samples **3-Y**. However, the electrochemical data relates only to a minor fraction of the bulk

(salen)Mn complexes, the total current uptake being much smaller than the amount of encapsulated complex.

In contrast, parallel EPR measurements indicated that in the bulk zeolite particles only about 20% of the Mn^{II} initially present in complexes **1-Y** and **2-Y** had been oxidized to Mn^{III}. This apparent discrepancy between electrochemical and EPR measurements indicates that the oxidation of Mn^{II} to Mn^{III} is only complete in the outermost layers, thus establishing a non-uniform distribution of manganese oxidation states through the zeolite grain.

Our work highlights the fact that, in the case of transition metal complexes encapsulated within zeolites, the catalytic behaviour could be due to a minor fraction of the total population residing in the outermost layers and having an oxidation state distinct from that of the bulk of the complex located deeper inside the zeolite particles.

Experimental Section

Preparation of Complexes 1-Y, 2-Y, and 3-Y: A mixture of 1 g of calcined and dehydrated Mn^{2+}-pre-exchanged zeolite Y (0.48% Mn^{2+}; measured by atomic absorption spectroscopy) and 0.150 g (0.56 mmol) of the previously synthesized ligand 1,2-bis(salicylideniminoethylene) was refluxed in 10 mL of dichloromethane for 12 h under nitrogen. The resulting yellow slurry was then refluxed for a further 12 h while air was bubbled through it. After filtration, the inorganic solid was subjected to Soxhlet extraction with dichloromethane for 8 h to remove excess complex and reactants. The solid was then treated with 10 mL of 1 M aq. NaCl solution for 4 h to afford the supported complex **1-Y**.

The preparation of **2-Y** was carried out by stirring 1 g of the supported complex **1-Y** with 0.02 g (0.173 mmol) of trimethylsilyl azide in 10 mL of dichloromethane for 12 h at room temperature under air bubbling. The heterogeneous complex **2-Y** thus obtained was collected by filtration and subjected to Soxhlet extraction with dichloromethane for 8 h to remove excess complex and reactants.

Sample **3-Y** was prepared through photochemical decomposition of the heterogeneous azide complex **2-Y**. The conversion could be followed by monitoring the disappearance of the characteristic IR azide stretching band and the concomitant increase of a Raman absorption at 1050 cm^{-1} assigned in the literature to the manganese(V) nitride triple bond that is progressively formed during the course of the irradiation.[11] The photolysis was carried out at room temperature in the solid state using self-supporting compressed pellets. These were irradiated through Pyrex (λ 300 nm) with light from a medium-pressure 125-W mercury lamp equipped with an outer jacket refrigerating system.

IR Spectra: FT-IR spectra of the complexes in the zeolites were recorded at room temperature using a greaseless CaF_2 cell in a Nicolet 710 FT spectrophotometer. Self-supporting wafers (ca. 10 mg) were prepared by compressing the zeolite powder at 1 $toncm^{-2}$. The samples were degassed at 100 °C and 10^{-2} Pa for 1 h prior to recording of the spectra.

EPR Spectra: Room-temperature EPR spectra were recorded with a Bruker ER200D spectrometer, working at the X-band (9.65 GHz) and using DPPH (g = 2.0036) as a reference standard. The total number of Mn^{II} ions was calculated by double integration of the signal and comparison of its area with that of the signal of the original Mn^{2+}-Y zeolite.

Electrochemical Measurements: Electrochemical measurements were performed in a conventional three-electrode cell at room temperature under argon. Cyclic voltammograms were obtained using a Newtronics 200P wave generator and an HQ 1000 potentiostat. Differential pulse voltammograms were recorded with a Metrohm E506 Polarecord.

Polymer-film electrodes were prepared as reported previously.[12a] A few μL of a dispersion of the zeolite (10 mg) in acetone (5 mL) was deposited onto the surface of a freshly polished glassy carbon electrode and the coating was allowed to dry in air at room temperature. Then, one drop of a solution of Palaroid B72 (Rohm Haas) in acetone was added and the modified electrode was dried in air. Palaroid provides a uniform thin film that exhibits good adherence and mechanical resistance.[12b]

Voltammograms of the pure complexes were recorded from 1−2 mM solutions in CH_3CN or DMSO using a freshly polished glassy carbon electrode (GCE). A platinum gauze pseudo-reference electrode was used for experiments in organic solvents, whereas a saturated calomel electrode (SCE) was used as a reference in aqueous solutions. All potentials mentioned in the text are referred to aqueous SCE. A platinum wire was used as an inert auxiliary electrode.

For experiments in organic solvents, Et_4NClO_4 (0.1 M) and Bu_4NPF_6 (0.1 M) were used as supporting electrolytes. For experiments in aqueous media, 0.15 M $NaClO_4$ was used.

XPS Measurements: XPS measurements were made at room temperature using a concentric hemispherical analyzer operated in the constant pass energy mode (50 eV). An Mg-K_α X-ray source (hν = 1253.6 eV) was used. A vacuum of ca. 5×10^{-9} Torr in the analysis chamber was maintained throughout the XPS recording. Charging effects were calibrated by analysis of the C (1s) line at 284.6 eV.

Acknowledgments

Financial support from the Spanish DGICYT (H. G., MAT97−1016-CO2) and the Generalitat Valenciana (M. J. S., GVDOC99−0203) is gratefully acknowledged.

[1] D. E. De Vos, P. Knops-Gerrits, R. F. Parton, B. M. Weckhuysen, P. A. Jacobs, R. A. Schoonheydt, *J. Incl. Phen. Mol. Recog. Chem*. **1995**, *21*, 185−213.
[2] N. Herron, *Inorg. Chem.* **1986**, *25*, 4714−4717.
[3] K. J. Balkus, A. G. Gabrielov, *J. Incl. Phen. Mol. Recog. Chem*. **1995**, *21*, 159−184.
[4] E. N. Jacobsen, W. Zhang, *J. Org. Chem.* **1991**, *56*, 2296−2298.
[5] [5a] S. B. Ogunwumi, T. Bein, *Chem. Commun.* **1997**, 901−902. − [5b] M. J. Sabater, A. Corma, A. Doménech, V. Fornés, H. García, *Chem. Commun.* **1997**, 1285−1286. − [5c] C. Bowers, P. K. Dutta, *J. Catal*. **1990**, *122*, 271−279.
[6] S. P. Varkey, C. Ratnasamy, P. Ratnasamy, *J. Mol. Catal*. **1998**, *135*, 295−306.
[7] P. Piaggio, P. McMorn, C. Langham, D. Bethull, P.C. Bulmanpage, F. E. Hancock, G. J. Hutchings, *New J. Chem*. **1998**, 1167−1169.
[8] F. Bedioui, L. Roue, J. Devinck, K. J. Balkus, Jr., *Stud. Surf. Sci. Catal*. **1994**, 917−924.
[9] L. Gaillon, N. Sajot, F. Bedioui, J. Devynck, *J. Electroanal. Chem*. **1993**, *345*, 157−167.
[10] C. Senaratne, J. Zhang, M. D. Baker, C. A. Bessel, D. L. Rolison, *J. Phys. Chem.* **1996**, *100*, 5849−5862.
[11] P. Formentín, J. V. Folgado, V. Fornés, H. García, F. Márquez, M. J. Sabater, *J. Phys. Chem. B*, submitted.
[12] [12a] A. Doménech, I. Casades, H. García, *J. Org. Chem.* **1999**, *64*, 3731−3735. − [12b] J. M. Kauffmann, T. Montenez, J. L. Vandenbalck, G. I. Patriarche, *Mikrochim. Acta* **1984**, 95−105.

[13] [13a] J. L. Leighton, E. N. Jacobsen, *J. Org. Chem.* **1996**, *61*, 389−390. − [13b] J. F. Larrow, E. N. Jacobsen, *J. Org. Chem.* **1994**, *59*, 1939−1942.
[14] F. Bedioui, E. De Boysson, J. Devynck, K. J. Balkus, Jr., *J. Chem. Soc., Faraday Trans.* **1991**, *87*, 3831−3834.
[15] F. Bedioui, L. Roué, E. Briot, J. Devynck, S. L. Bell, K. J. Balkus, Jr., *J. Electroanal. Chem*. **1994**, *373*, 19−29.
[16] [16a] C. P. Horwitz, S. E. Creager, R. W. Murray, *Inorg. Chem.* **1990**, *29*, 1006−1011. − [16b] F. Bedioui, E. Labbe, S. Gutierrez-Granados, J. Devynck, *J. Electroanal. Chem*. **1991**, *301*, 267−274.
[17] The theoretical response as a function of the relative Mn^{III}/Mn^{II} population was generated using the SIMULA (10) program. Comparison with theoretical curves is feasible since it has been observed that these plots depend on the scan rate, the Mn^{III}/Mn^{II} ratio, as well as the initial and switching potentials.
[18] Mn^{III} is EPR inactive, hence it has been quantified by assuming that the increase in this species corresponds to the decrease in Mn^{II}, as estimated from the area of the EPR signal before and after oxidative treatment.
[19] [19a] M. J. Sabater, S. García, M. Alvaro, H. García, J. C. Scaiano, *J. Am. Chem. Soc.* **1998**, *120*, 8521−8522. − [19b] P. Knops-Gerrits, D. De Vos, F. Thibault-Starzyk, P. A. Jacobs, *Nature* **1994**, *369*, 543−546.
[20] M. J. Sabater, A. Corma, J. V. Folgado, H. García, *J. Phys. Org. Chem.* **2000**, *13*, 57–62.

Received October 19, 1999
[I99367]